Time-Based Compression and Classification of Heartbeats

Alexander Singh Alvarado*, Choudur Lakshminarayan, and José C. Príncipe, *Fellow, IEEE*

***Abstract*—Heart function measured by electrocardiograms (ECG) is crucial for patient care. ECG generated waveforms are used to find patterns of irregularities in cardiac cycles in patients. In many cases, irregularities evolve over an extended period of time that requires continuous monitoring. However, this requires wireless ECG recording devices. These devices consist of an enclosed system that includes electrodes, processing circuitry, and a wireless communication block imposing constraints on area, power, bandwidth, and resolution. In order to provide continuous monitoring of cardiac functions for real-time diagnostics, we propose a methodology that combines compression and analysis of heartbeats. The signal encoding scheme is the time-based integrate and fire sampler. The diagnostics can be performed directly on the samples avoiding reconstruction required by the competing finite rate of innovation and compressed sensing. As an added benefit, our scheme provides an efficient hardware implementation and a compressed representation for the ECG recordings, while still preserving discriminative features. We demonstrate the performance of our approach through a heartbeat classification application consisting of normal and irregular heartbeats known as arrhythmia. Our approach that uses simple features extracted from ECG signals is comparable to results in the published literature.**

***Index Terms*—Electrocardiograms (ECG) classification, electrocardiograms (ECG) compression, event-based representation, heartbeat classification, integrate and fire (IF).**

I. Introduction

ACCORDING to the World Health Organization (WHO) cardiovascular diseases (CVDs) are the leading causes of death and disability in the world. An estimated 17.3 million people died from CVDs in 2008, representing 30% of all global deaths [1]. Furthermore, in 2010, heart related diseases cost the healthcare industry in the United States $316.4 billion. This total includes the cost of health care services, medications, and lost productivity [2]. Although a large proportion of CVDs are preventable, they continue to rise mainly because preventive measures are inadequate. Electrocardioagram (ECG) is a standard tool to monitor heart function. Although access to ECG is readily available, patients with compromised heart function require continuous monitoring. Regular monitoring of ECG helps in early detection of irregularities in the heartbeats. Some heartbeat arrhythmias, although not immediately life threatening, may need timely detection and attention to prevent future complications. In order to provide continuous health monitoring, devices must integrate seamlessly into the patients life and not interfere with daily activities. Toward this goal, wireless body area networks (WBANs) have become an emerging technology [3], [4]. These networks consist of a number of physiological sensors that monitor the patients vital signs. Unlike conventional Holter monitors that record the heartbeat rhythms and process the data offline [5], WBAN are designed to provide real-time diagnostics. Current wireless ECG systems can be grouped into two broad categories [6], [7]: those with wired sensors and those with wireless sensors. The first group [6] connects a single wireless transmitter to all the sensors by a set of wires. This approach still requires bulky equipment and introduces movement artifacts and noise. The second group integrates the sensor and the wireless transmitter, providing the patient greater mobility and potentially 24/7 monitoring [8]. The main challenges of these systems include power, area, bandwidth, and quality of the recording.

In order to satisfy the bandwidth constraints a number of compression methods have been proposed in the literature (wavelet decompositions, spectral coefficients, and others). These compression algorithms are applied to data that has been sampled uniformly at a rate above the Nysquist bound. The samples are then compressed to reduce the data rates. The downside being that these solutions lead to bulky circuits, which consume area and power.

Novel sampling methods merge both the compression and sampling stages by lifting the bandlimitedness assumption and working directly with sparse representations of the input. This includes the work in compressive sensing (CS) [9] and finite rate of innovation (FRI) [10]. Both these methods assume a specific sparsity or degrees of freedom on the input, which may change through time depending on the shape of the heartbeat cycles. Furthermore, the basis functions are stochastic, the signal structure is spread across the full space, which means that it is very unlikely to extract features in this space that will lead to classifiers without doing the reconstruction. Finally, they have not been designed with low power hardware constraints.

In order to satisfy all constraints (bandwidth, area, power, and resolution), we propose a time-based encoding scheme for ECG

Manuscript received December 4, 2011; revised February 2, 2012; accepted February 28, 2012. Date of publication March 20, 2012; date of current version May 18, 2012. This work was supported by the Hewlett-Packard Laboratories (HP Labs) under the Innovation Research program Contract CW221761. *Asterisk indicates corresponding author.*

*A S. Alvarado is with the Department of Electrical and Computer Engineering, University of Florida, Gainesville, FL 32611 USA (e-mail: asingh@cnel.ufl.edu).

C. Lakshminarayan is with the Hewlett-Packard Laboratories, Palo Alto, CA 94304 USA (e-mail: choudur.lakshminarayan@hp.com).

J. C. Príncipe is with the Department of Electrical and Computer Engineering and the University of Florida Computational Neuro-Engineering Laboratory, University of Florida, Gainesville, FL 32611 USA (e-mail: principe@cnel.ufl.edu).

Color versions of one or more of the figures in this paper are available online at http://ieeexplore.ieee.org.

Digital Object Identifier 10.1109/TBME.2012.2191407

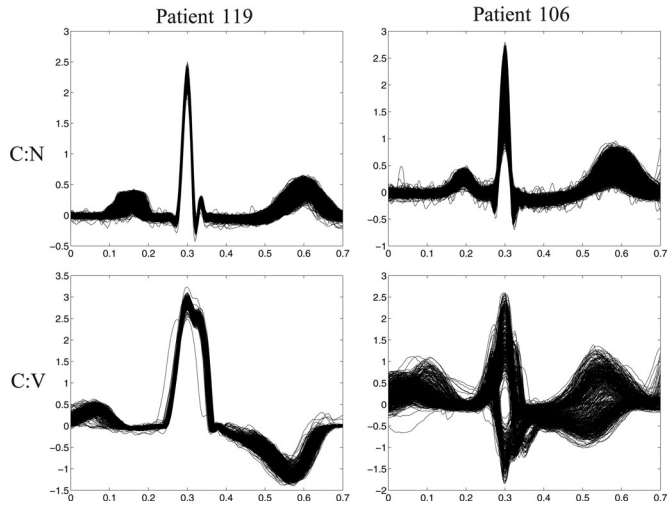

Fig. 1. Example of heartbeat shapes from the MIT-BIH dataset. Each column represents a patient and each row the beats for that specific class (using the class numbering from Table I). Note the variations in the beat morphology across patients as well as within a patient.

recordings, based on the integrate and fire (IF) sampler [11]. This sampler has been shown to provide accurate and compressed representations of a similar signal class (neural recordings [12]), along with an efficient hardware implementation [13].

In this paper, we use time based encodings of the ECG recordings to perform the classification of normal heartbeats and irregular heartbeats known as arrhythmias. We use the time-based representation directly to extract discriminative features, avoiding reconstruction all together. In order to compare the performance of our method with those in the published literature, we use the classifier described by Chazal and Reilly [14]. We differ from [14] in that the features are extracted from the output of an IF sampler. While, the active learning approach presented in [15] outperforms our method, the pulse-based features can be used in their framework.

This paper is organized as follows: first, Section II describes the classification problem for ECGs and Section III provides the description of the recordings. Section IV introduces the IF sampler and Section V describes the classifier based on the output pulses from the IF. Section VI defines the performance metrics used and finally, Section VII presents classification and data rate results based on the MIT-BIH arrhythmia database.

II. Heartbeat Classification

Classification of ECG signals is a very difficult problem and current research is focused on careful extraction of heartbeat features. A major problem encountered by machine learning techniques for classifying ECG signals is due to the large interpatient and intrapatient variability in the timing profiles and morphology of damaged cardiovascular processes (see Fig. 1). The effect of this behavior is that classifiers trained using traditional methods fail when applied to new patients. Several approaches have been proposed. Hu *et al.,* [16] used a mixture of experts approach that combines global and local classifiers. The global classifier uses heartbeat signatures from a vast collection of labeled data. The local classifier trains on patient-specific ECG recordings. A gating function weights the classification results of the global and local experts and combines them to make a decision. Chazal and Reilly [14] proposed an approach based on heartbeat morphology features, heartbeat interval features, and RR interval features and utilizes the linear discriminant analysis (LDA) for classification. Ince *et al.,* [17] proposed a patient-specific classification methodology for accurate classification of heartbeat patterns. Wiens and Guttag [15] proposed active learning that reduces the amount of patient-specific (annotated) data needed for classification. It is, therefore, evident that heartbeat classification researches have focused exclusively on patient-specific ECG signatures and features.

Our approach is to analyze the ECG signals using the stream of pulses generated by the IF sampler, extract the pulse features based on the precise timing of these events, and evaluate classifier performance. Therefore, the ECG signal does not need to be reconstructed, at least for classification. We choose the LDA following [14]. Needless to say, our approach achieves the dual purpose of compressing the data intensive ECG signals, and performing classification in the pulse domain. While, ECG data compression has been done in the past using FRI and CS, these approaches require knowledge of the sparsity of the signal. Heartbeat cycles, however, are regularly paced, but arrhythmia conditions induce irregularities such that knowledge of signal sparsity *a priori* may be unknown. Furthermore, signal analysis still requires reconstruction. We propose the IF sampler because the heartbeat cycles are localized in time and amplitude and many forms of arrhythmias are discernible irregularities near the QRS complex in the heartbeat cycle. Furthermore, the output pulse distribution (generated by IF) is input dependent and it adapts to changes in the heartbeats shapes or rhythms. Thus, our proposal is a holistic approach to tackle the problem of compression and classification of heartbeats that we believe can circumvent the bandwidth and real-time analysis bottlenecks to improve on-time delivery of healthcare to mitigate heart related fatalities. Results from our approach are comparable to state of the art.

III. Data Description

In order to test both compression and discriminability of heartbeats from ECG recordings of our method, we leveraged the standard MIT-BIH arrhythmia database [18]. The database consists of 48 fully annotated, 30 min, two-lead ECG recordings from 47 different patients (recordings 201 and 202 are from the same patient). The leads usually involve the modified limb lead II (MLLII) and one of the modified leads V1, V2, V4, or V5 [18]. Since the second lead usually varies for each recording (patient), all the results in this paper are based on the MLLII. The data are sampled at 360 Hz and the ± 5 mV range is quantized to 11 bits.

Unfortunately a number of artifacts such as power line interference, contact noise, motion, electromyographic noise, and baseline drift compromise the quality of recordings [19]. In order to attenuate the effect of these artifacts the recordings were preprocessed as described in [14], [15], and [20]:

TABLE I
HEARTBEAT CLASSES GIVEN BY THE MIT-BIH DATABASE ALONG WITH THE REGROUPING DEFINED BY THE AAMI STANDARD

MIT-BIH class	MIT-BIH number	Number of Samples	AAMI groups	Number of samples.
Normal beat	1	75052	N: Beats not found in the class S, V, F and Q.	90631
Left bundle branch block beat	3	7259		
Right bundle branch block beat	2	8075		
atrial escape beats	34	16		
Nodal (junctional) escape beat	11	229		
Atrial premature beat	8	2546	S: Supraventricular ectopic beat.	2781
Aberrated atrial premature beat	4	150		
Nodal(junctional) premature beat	7	83		
Supraventricular premature beat	9	2		
Premature ventricular contraction	5	7130	V: Ventricular ectopic beat.	7236
Ventricular escape beat	10	106		
Fusion of ventricular and normal beat	6	803	Fusion beat (F)	803
Paced beat	12	7028	Q: Unknown beat.	8043
Fusion of paced and normal beat	38	982		
Unclassified beat.	13	33		

1) First, the data are passed through a median filter with window size 200 ms that removes the P-waves and QRS complexes [21].
2) A second median filter with window size 600 ms, removes the T-waves.
3) The filtered signal represents the baseline that is then subtracted from the original recording.
4) Finally, a notch filter centered at 60 Hz is implemented through a 60-tap finite impulse response filter, in order to remove power line interference.

The top panel in Fig. 3 shows a short segment of the raw ECG recordings and the processed version. The MIT-BIH database includes a number of examples for different rhythms, QRS morphology, and signal quality, for a review on the fundamentals of ECG recordings refer to [21]. In this paper, we are only concerned with the heartbeat annotations. Most of these labels are placed at the peak of the R-wave of each beat, although some are misaligned. When the peak of the R-wave is misaligned in the heartbeat cycle, we search for the local maxima and adjust for the R-wave timing. We extract windows of 700 ms around the beat, 300 ms before, and 400 ms after the R-peak annotations.

The beats in the MIT-BIH database are classified into 20 classes. The literature uses a number of different clusterings of the data in order to test heartbeat classifiers. However, we will use the standard defined by the Association for the Advancement of Medical Instrumentation (AAMI) [22]. Table I shows the labels provided by the MIT-BIH database and how they are reclustered according to the AAMI standard.

According to the AAMI standard, although there are five designated classes, the classification problem is decomposed into two binary classifications tasks. The first task consists of distinguishing ventricular ectopic beat (V) against the remaining classes (N, S, F, Q). The second classification task consists of detecting S versus the classes (N, V, F, Q).

In order to perform the classification using LDA in a supervisory mode, we create training and testing datasets. As mentioned in the introduction, patient-specific heartbeat signals have been shown to improve classification accuracy. Following the approach presented in [14], the classification is based on a global and a local classifier discussed in Section V. The training data relative to the global classifier is the set $\mathcal{T}$ consisting of patient records given as follows:

$$\mathcal{T} := \{101, 106, 108, 109, 112, 114, 115, 116, 118, 119, 122, 124, 201, 203, 205, 207, 208, 209, 215, 220, 223, 230\}.$$

Each item in the set $\mathcal{T}$ is a patient identification number designated in the MIT-BIH arrhythmia database. The testing dataset consists of the remaining patients records from the MIT-BIH arrhythmia database

$$\mathcal{V} := \{100, 103, 105, 111, 113, 117, 121, 123, 200, 202, 210, 212, 213, 214, 219, 221, 222, 228, 231, 232, 233, 234\}.$$

Since each patient's unique beat morphology contributes to prediction accuracy, a sample of heartbeats of a patient in the testing set $\mathcal{V}$ is appended to the set $\mathcal{T}$. For example, in order to label a sequence of heartbeats of patient 100 in $\mathcal{V}$, the first five hundred beats are added to the set $\mathcal{T}$. In the next step, the global and local classifiers trained with the data in $\mathcal{T}$ and the patient-specific set of 500 beats, respectively. Finally, the remaining heartbeats (excluding the first 500) for the patient are classified using the global-local classifier pair. These steps are repeated for all the patients in $\mathcal{V}$ to determine overall accuracy of the method.

IV. INTEGRATE AND FIRE SAMPLER

The IF model is well known in the computational neuroscience literature and similar samplers have been proposed in the past [23], [24], specially in connection with the well known, discrete, continuous time, and asynchronous $\Sigma - \Delta$ modulators [25]. Nevertheless, these samplers have not been designed with compression or hardware constraints in mind and, therefore, the generated sample distributions are usually not sparse and compression is lost.

The block diagram of the IF sampler is shown in Fig. 2. The input signal x is convolved with an averaging function u and the output is then compared against two thresholds $\{\theta_p, \theta_n\}$. Once the aggregated signal equals or exceeds the threshold a pulse is generated at that time instant and the integrator is reset and held their for a specific duration known as the refractory period and denoted by τ. Note that the refractory period can be adjusted to limit the pulse rates independently from the input. Assuming

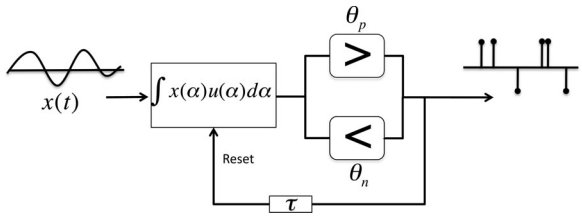

Fig. 2. IF block diagram.

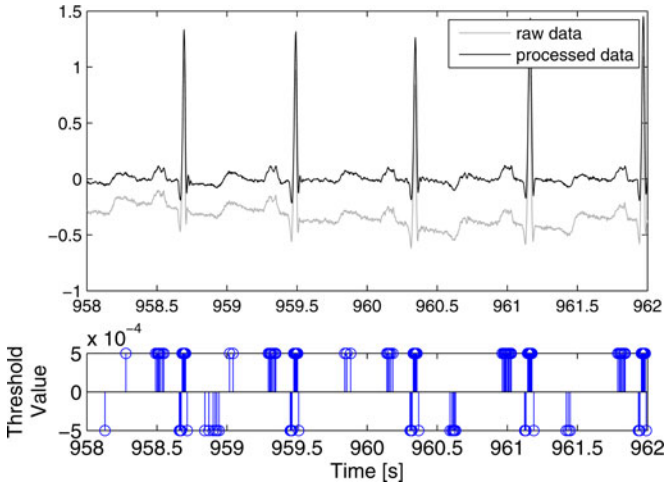

Fig. 3. Example of heartbeat shapes from the MIT-BIH dataset for patient 100. The top panel shows both the raw data and the processed data following the filter proposed in [14]. The bottom panel shows the pulses generated by the IF sampler, the average pulse rate along the entire recording is 40.59 pulses/s.

that the support of the signal x is compact, starting at t_0 we can define the pulse timings recursively. Note that the term $u(t)$ represented by $e^{\alpha(t-t_{k+1})}$ corresponds to the leaky factor in the integration:

$$\theta_k = \int_{t_k+\tau}^{t_{k+1}} x(t)e^{\alpha(t-t_{k+1})}dt \quad \theta_k \in \{\theta_p, \theta_n\} \tag{1}$$

where $\alpha, \tau > 0$, since the number of samples and their location is input dependent they provide a compressed representation for signals in which information is localized in high-amplitude transients overlaid on low-amplitude background noise. This is the case of ECG recordings, similar to neural signals [12]. Nevertheless, it is not straightforward to operate directly on the pulse trains. For example, addition and multiplication of pulse trains is not well defined and, therefore, a reconstruction algorithm [11], [12], [26] is typically used, in order to create a more amenable representation. We have shown that the reconstruction error can be bounded in bandlimited spaces [11] and perfect recovery is possible in finite-dimensional spaces, as long as the sample constraints are satisfied [12].

The bottom panel in Fig. 3 shows an example of a typical normal beat and the corresponding pulse representation. As we would expect the samples are localized in the QRS complex.

V. Pulse-Based Classification

The output pulses from the IF do not fall into standard representations used in signal processing, mainly because pulse trains are not easily represented in vector spaces. A number of different representations for pulse trains have been suggested in the computational neuroscience literature, these include stochastic point process models [27], projections into reproducing kernel Hilbert spaces [28], linear filtering [29], time embeddings based on the interpulse intervals [30], [31] and others [32], [33]. Throughout this paper, we use a simple binning approach, which is commonly used in the computational neuroscience literature [34]. We will show that this simple and computationally effective (integer addition) approach is sufficient to obtain classification results comparable to those reported in [14]. Nevertheless, in our future work, we will explore other representations for pulse trains that would allow us to classify them.

A. Pulse Preprocessing

Assuming a pulse train defined on the interval $[0, T]$, binning consists of dividing the domain into a set of nonoverlapping intervals and counting the number of events in each interval. These counts represent the binned vector. This representation maintains the temporal structure of the pulse while providing a vector space representation. Nevertheless, the precise timing is lost. A smaller bin size would reduce the time jitter but results in a higher dimensional space that would require more samples in a classification task. Here, we use a bin size of 35 ms, which was chosen experimentally from Fig. 4.

Since the heartbeats are limited in duration, we can represent them as an N-dimensional vector, where N is the number of bins. Fig. 1 shows the overlaid heartbeats for classes 1 (N) and 5 (V) for two different patients (119 106). The variability in the shapes for the same patient and across patients is evident specially in the case of class (V). Nevertheless, the shape of the heartbeats is not sufficient in some cases to discriminate the classes. Therefore, information on the pre- and post-RR intervals is included. In order to use this feature across patients, a normalization step is required, as suggested in [14] we use both the pre- and post-RR intervals as well as the pre- and post-RR intervals normalized by the mean RR-interval for the specific patient. Nevertheless, this paper is only concerned with the discrimination power of the proposed pulse-based representation and, therefore, we assume the location of the beats is given. The problem of detection will be treated in future work.

The feature vector for any given beat consists of N counts followed by pre- and post-RR intervals with and without normalization. This produces an $(N + 4)$-dimensional feature vector that is then fed into the classifier.

B. Classifier

A number of different classifiers have been used in the literature including, SVM [35], postclassification following clustering, LDA [14], fuzzy networks, phase space reconstruction [36], [37], and others. Chazal and Reilly [14] proposed classification based on the LDA [38]

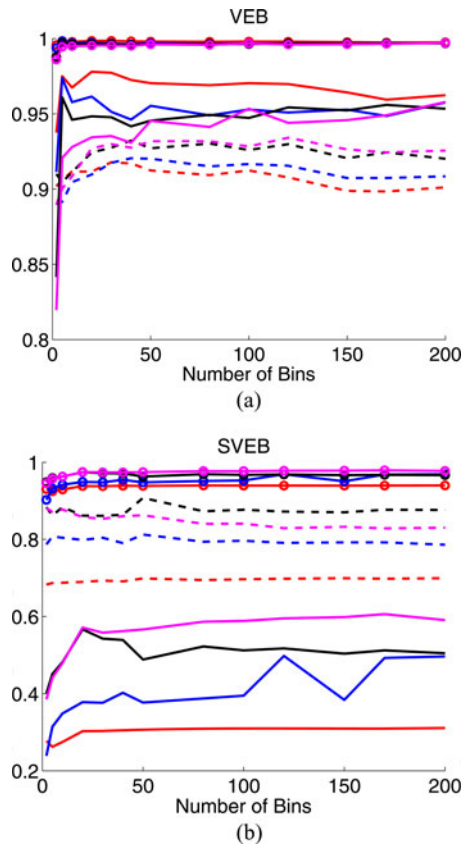

Fig. 4. Plot of the classification metrics for both VEB and SVEB classes in relation to the number of bins used to create the feature vector, as well as the pulse rates. The color of the lines correspond to the different pulse rates (red = 29.76, blue = 63.88, black = 117.86, and magenta = 223.34). The line types correspond to three metrics, the solid lines represent PPV, the dashed lines are sensitivity and the lines with the circular markers are specificity. Throughout this paper, we fixed the number of bins equal to 20, which corresponds to a bin width of 35 ms and the heartbeat range parameter W is set to 0.7 s. (a) VEB (V). (b) SVEB (S).

classifier. We implement the LDA using features extracted from the pulses generated by the IF sampler. Classification by LDA is based on the posterior probability of class membership of a new example. Also, LDA assumes that the underlying probability density function of the data is Gaussian. More formally, the posterior probability of an example x belonging to class k is

$$P(k|x) = \frac{P(x|k)P(k)}{P(x)} \tag{2}$$

where $P(x|k)$ is the class conditional distribution of the feature vector x (note that this distribution parametrizes the distribution of a heartbeat belonging to class k, $P(k)$ is the prior distribution of class k (the probability of class k, which is merely the proportion of heartbeat samples belonging to class k, and $P(x)$ is the marginal distribution of the sample features.

Since the marginal distribution $P(x)$ is common across all classes, it is often dropped from the decision function. Here, $k \in \{1, \ldots, c\}$ indexes the class, c the number of classes, and x represents the feature vector. In the following, we will parametrize the different components involved in the posterior density function $P(k|x)$. Under the Gaussian assumption of the feature vector x, the sampling distribution $P(x|k)$ is rewritten as

$$P(x|k) = \frac{1}{|\Sigma|^{\frac{1}{2}}(2\pi)^{\frac{p}{2}}} \exp\left(-\frac{1}{2}(x-\mu_k)^T \Sigma_p^{-1}(x-\mu_k)^T\right) \tag{3}$$

where $\mu_k, k \in \{1, \ldots, c\}$ are the class conditional means, and Σ_p is the pooled covariance matrix and is given by

$$\Sigma_p = \sum_k^c \omega_k \Sigma_k \tag{4}$$

where the weights ω_k where chosen as in [14]. Correspondingly N: 400/1608; S: 400/1608; V: 400/1608; F: 400/1608; Q: 8/1608. The prior distribution $P(k)$ is π_k, and the distribution $p(x)$ is given by

$$p(x) = \sum_{k=1}^{c} P(x|k)P(k). \tag{5}$$

The decision rule $d_k(x)$ to determine membership of a new vector x is given by

$$d_k(x) = \underbrace{\operatorname{argmax}}_{k} P(k|x). \tag{6}$$

As $P(k|x)$ is positive, we may as well use the logarithm of the $P(k|x)$ since it does not affect the decision. Therefore, using the Gaussian probability density function and taking logarithms, we have

$$\log(P(k|x)) \approx C - \frac{1}{2}(x-\mu_k)^T \Sigma_p^{-1}(x-\mu_k)^T + \log \pi_k \tag{7}$$

where C is a constant. The quantities μ_k, Σ_k, and π_k are learned from the training set *a priori* and are plugged into (7) to evaluate the decision rule. Given a new example x_{new}, its membership is determined by finding the largest $d_k, k \in \{1, \ldots, c\}$. If the prior probabilities π_k are assumed to be equal, the $\log \pi_k$ term in the decision rule may be dropped. In this case, the priors are selected as in Chazal and Reilly [14]. The prior probability of the N, S, V and F classes was set to $10/41$, while the prior probability of the Q class was set to $1/41$.

In the classification of patient heartbeats, due to the inherent variability across and within patients, a test patient's unique heartbeat data are combined with the global set of features of all patients to perform classification. Therefore, the training set is dependent on the test patient. Intuitively training samples from the test patient (a.k.a local training set) should be given higher importance than those in the global training set. In order to do so Chazal and Reilly [14] suggests learning the parameters for two LDA classifiers, based on local (μ_k^l, Σ_k^l) and global (μ_k^g, Σ_k^g) parameters estimated from the training sets. The estimated parameters are then combined linearly, such that

$$\mu_k = K_k \mu_k^g + (1-K_k)\mu_k^l \tag{8}$$

$$\Sigma_k = K_k \Sigma_k^g + (1-K_k)\Sigma_k^l. \tag{9}$$

Given that we only have access to a short segment of the ECG, it is conceivable that certain beat classes may not appear in the local training set. In such a scenario the local set is not useful

TABLE II
CLASSIFICATION RESULTS USING THE BINNED PULSE FEATURES (20 BINS) FOR EACH OF THE TEST PATIENTS

	Number of Beats					SVEB			VEB			
Rec	N	S	V	F	Q	ACC	SE	PPV	ACC	SE	PPV	Average sample rate
100	1744	28	1	0	0	95.93	53.57	20.27	100.00	100.00	100.00	40.59
103	1582	2	0	0	0	99.74	0	0	100.00	-	-	93.44
105	2041	0	26	0	5	93.62	-	0	94.24	88.46	16.54	157.00
111	1623	0	1	0	0	99.81	-	0	99.93	0	-	101.70
113	1293	2	0	0	0	100.0	100.00	100.00	100.00	-	-	118.40
117	1034	1	0	0	0	99.71	0	0	99.90	-	0	89.28
121	1361	1	1	0	0	93.83	100.00	1.17	99.92	0	-	47.23
123	1016	0	2	0	0	99.90	-	0	100.00	100.00	100.00	78.79
200	1390	28	681	2	0	94.66	32.14	8.82	96.76	90.01	100.00	144.70
202	1569	54	12	1	0	85.88	79.62	16.34	99.93	91.66	100.00	81.25
210	1959	20	162	9	0	98.83	85.00	43.58	98.83	85.18	99.28	93.87
212	2248	0	0	0	0	99.77	-	0	99.86	-	0	165.60
213	2252	27	199	273	0	98.82	3.70	14.28	99.11	89.44	98.34	327.80
214	1564	0	197	1	0	99.37	-	0	99.37	94.92	99.46	172.70
219	1604	3	47	0	0	97.52	0	0	99.15	72.34	97.14	133.00
221	1626	0	301	0	0	99.84	-	0	99.68	98.00	100.00	93.48
222	1774	209	0	0	0	83.96	59.80	34.81	100.00	-	-	45.25
228	1300	3	250	0	0	99.48	0	0	99.42	97.20	99.18	100.50
231	1071	0	0	0	0	99.81	-	0	100.00	-	-	104.80
232	271	1009	0	0	0	99.29	99.60	99.50	99.92	-	-	69.99
233	1873	4	696	6	0	99.30	100.00	18.18	98.56	94.68	100.00	243.10
234	2200	50	3	0	0	98.49	40.00	83.33	99.82	0	0	89.52

Column 1 refers to the record number as assigned in the MIT-BIH database, columns 2–6 represent the number of beats per class, columns 7–12 represent the performance metrics and column 13 shows the average sample rate from the time-encoded record. The average results for all metrics along all patients are presented in Table IV as the row in bold.

and may be ignored. Operationally, we use a parameter K_k that weighs the local and global classifiers, respectively, given in (10). The parameter K_k is determined in relation to the number of samples in a given class as suggested in [14]:

$$K_k = \min\left\{\frac{N_k^g}{10}, W\right\} \tag{10}$$

where N_k^g is the number of samples in class k and the parameter W is usually set to 0.7.

VI. PERFORMANCE METRICS

We measure the performance of our methodology in terms of overall sample rates and the classification error. The data rates are varied by changing the thresholds θ_p, θ_n of the IF sampler. For each threshold, all 48 records are transformed into pulse trains and the average pulse rate is reported. The classification results are tabulated in terms of the sensitivity SE_i, specificity SP_i, positive predictive value PPV_i, and accuracy ACC_i which are, respectively, defined as follows:

$$\mathrm{SP}_i = \frac{\mathrm{TN}_i}{\mathrm{TN}_i + \mathrm{FP}_i}, \quad \mathrm{PPV}_i = \frac{\mathrm{TP}_i}{\mathrm{TP}_i + \mathrm{FP}_i} \tag{11}$$

$$\mathrm{SE}_i = \frac{\mathrm{TP}_i}{\mathrm{TP}_i + \mathrm{FN}_i}, \quad \mathrm{ACC}_i = \frac{\mathrm{TP}_i + \mathrm{TN}_i}{\mathrm{TP}_i + \mathrm{TN}_i + \mathrm{FP}_i + \mathrm{FN}_i} \tag{12}$$

where TP_i (true positive) is the number of beats of the ith class correctly classified; TN_i (true negative) is the number of beats not belonging to the ith class and not classified in the ith class; FP_i (false positive) number of beats erroneously classified into the ith class; and finally FN_i (false negatives) is the number of beats of the ith class classified into a different class. The accuracy ACC_i, denotes the ratio between all correctly and incorrectly classified beats.

VII. RESULTS AND DISCUSSION

Evaluation of classifier performance is reported using the MIT-BIH arrhythmia database and in accordance with the AAMI standard. The results of binary classification tests-VEB (V) versus (N, S, F, and Q) and SVEB (S) versus (N, V, F, and Q) are reported and tabulated in Table II. Each row corresponds to a test patient whose record number is given in column 1, columns 2–6 correspond to the number of beats in each class, columns 7–12 present the classification results in terms of accuracy ACC, sensitivity SE, and predictive positive value PPV. Finally, column 13 displays the average sample rate. As the feature vector for classification is based on pulse counts in each bin, we determined the number of bins to be 20. Fig. 4 shows the effects of varying the number of bins as a function of the classification metrics at different pulse rates. It is noteworthy that size of the bin does not play a crucial role, which suggests that the finer details in the heartbeat shapes do not provide extra information for discriminability purposes. While the AAMI standard for classification of heartbeats insists on analysis involving two classes (the VEB and SVEB classes against the bundled classes (N, F, Q, S/V), we also report results obtained by considering each of the five classes in the AAMI recommended taxonomy (S, N, V, F, and Q)as a stand-alone class. In other words, we measure the performance of the LDA across five classes. Table III consists of the results averaged over all patients. Comparing the results against those tabulated in Table V in [14]. The performance of the two procedures track each other across all classes. There are indeed some variations in the performances of the classifiers across the five heartbeat classes, notably the misclassification of normal beats (N) into the SVEB (S) class is significantly higher for the state of the art (1360), while our algorithm produces fewer false positives (844). But the situation is reversed relative to the classification of normal beats (N) to the class known

TABLE III
OVERALL CLASSIFICATION RESULTS USING THE BINNED PULSE FEATURES (20 BINS)

		Algorithm				
		N	S	V	F	Q
Reference	N	32415	844	127	829	180
	S	173	1242	3	10	13
	V	22	101	2384	63	9
	F	58	4	35	194	1
	Q	0	1	3	0	1

The threshold was selected such that the pulse rate was 117.86 pulses/s. These results are comparable to those presented in Chazal and Reilly [14]. The Reference title in the table corresponds to the actual heartbeat labels and the algorithm title correpsonds to the predicted labels.

TABLE IV
AVERAGE CLASSIFICATION METRICS COMPARED TO THE STATE OF THE ART

Methods	SVEB			VEB			Sample Rate
	SE	SP	PPV	SE	SP	PPV	
Hu et al. [16]	78.9	96.8	75.8	N/A	N/A	N/A	180
Chazal et al [14]	87.7	96.2	47.0	94.3	99.7	96.2	360
Ince et al. [17]	63.5	99.0	53.7	84.6	98.7	87.4	360
Wiens et al. [15]	92.0	100	99.5	99.6	99.9	99.3	128
Proposed	68.97	93.84	30.26	91.15	99.85	97.79	29.76
	79.87	94.91	37.78	90.96	99.73	96.14	63.88
	86.19	**97.45**	**56.68**	**92.43**	**99.6**	**94.82**	**117.86**
	85.77	97.5	57.14	92.71	99.53	93.43	223.34

The sample rates in the proposed method is the average over all patients.

as fusion beats (F). Survey and comparison of the tables shows alternating classifier performances across the classes, but overall the two algorithms produce similar results. More precisely, the overall classification rate obtained from Table V from Chazal *et al.,* is 93.8% while, we report an overall rate of 93.6%. Clearly, the classification rates due to the two algorithms is statistically insignificant. In conclusion, it is clear that our approach is able to emulate the state of the art, while maintaining a significantly lower sampling rate. In this case, an average sampling rate of 114 samples/s versus 360 samples/s (Chazal and Reilly [14]), which is a gain of a factor of three.

In our experimental setup, the IF sampler parameters were selected such that $\alpha = 100, \theta_p = 0.0005, -\theta_n = 0.0005, \tau = 1$ ms. These parameters were fixed through all the experiments. From the last column (average sampling rate) in Table II, it is evident that there is a large variation in the sampling rates. Nonetheless, for patient records 100 and 221, we obtain compression and discriminability for the SVEB and VEB classes, respectively. Furthermore, Table IV shows the average results over all the test patients for different average sample rates. These sample rates were obtained by varying the thresholds (θ_p and θ_n). Specifically, we compare our results to those from Chazal and Reilly [14] since both preprocessing and classifier are identical. Therefore, any discrepancy is due to the features that describe the heartbeat shapes. Comparing the row in bold (see Table IV) for which the average sample rate is 117.86 (note that Chazal and Reilly [14] uses 360 samples/s). Also, note that the classification results are comparable to those in [14], [16], and [17]. We have also added the results from Wien and Guttag [15] for completeness. These results cannot be directly compared to ours since the classification methodology is completely different. In [15], an active learning approach is presented in which the classifier has access to all the test beats (without the labels). In contrast, we only use the first 500 beats (with labels) following [14]. We may point out that the pulse-based features can be used in an active learning framework.

In order to implement [15] requires an elaborate experimental setup and results will be reported in a future submission.

Our goal here was to show that the compressed representation contains sufficient discriminative information and at the same time we can access discriminative information directly in the pulse domain without having to reconstruct the signal that is the typical approach when combining compression and classification. In terms of compression, we see that we have reduced the sample rates for certain patients. It may be noted that comparison of our methodology to existing methods, such as CS [39], [40] or FRI [41], is not possible since their approaches are designed toward signal reconstruction. Furthermore, in the case of CS it is not clear how one could design a classifiers based on random projections used for compression. This may be feasible in the case of FRI, we are investigating methods to combine FRI based compression and classification.

VIII. CONCLUSION

We have shown that time-based representations generated by the IF sampler provide compression while still preserving discriminability in heartbeat shapes in patients. The proposed features are obtained directly from the compressed representation avoiding any reconstruction. This approach to compression and classification for heartbeats has not been treated in the literature to the authors knowledge.

The features presented here are based on simple pulse counts in the bins. In the future, we may draw from current results in point process theory that will allow us to model each class based on a class conditional intensity function constructed from the precise timings of the events that may be construed as events from a renewal process. Furthermore, these features can also be used in combination with the active learning framework that has been shown to reduce the number of labeled heartbeats required from an expert cardiologist.

ACKNOWLEDGMENT

The authors would like to thank I. Jekova and J. Wiens for insightful comments in understanding the fundamentals of heartbeat classification. We also thank K. Shrestha for comments and careful reading of the manuscript.

REFERENCES

[1] W. H. Organization. (2008, Nov.) Cardiovascular diseases. [Online]. Available: http://www.who.int/cardiovascular_diseases/en/ 2012.
[2] C. for Disease Control and Prevention. Heart disease facts. (2010). [Online]. Available: http://www.cdc.gov/heartdisease/facts.htm
[3] J. Luprano, J. Sola, S. Dasen, J. Koller, and O. Chetelat, "Combination of body sensor networks and on-body signal processing algorithms: the practical case of myheart project," in *Proc. Int. Workshop Wearable Implantable Body Sens. Netw.*, Apr. 2006, pp. 4–79.
[4] A. Volmer and R. Orglmeister, "Wireless body sensor network for low-power motion-tolerant syncronized vital sign measurment," in *Proc. 30th Annu. Int. Conf. IEEE Eng. Med. Biol. Soc.,* Aug. 2008, pp. 3422 –3425.
[5] Irhythm. The zio patch. (2011, Nov.) [Online]. Available: http://www.irhythmtech.com/

[6] A. Sapio and G. Tsouri, "Low-power body sensor network for wireless ECG based on relaying of creeping waves at 2.4 GHz," in *Proc. Int. Conf. Body Sens. Netw.*, Jun. 2010, pp. 167–173.
[7] H. Mamaghanian, N. Khaled, D. Atienza, and P. Vandergheynst, "Compressed sensing for real-time energy-efficient ecg compression on wireless body sensor nodes," *IEEE Trans. Biomed. Eng.*, vol. 58, no. 9, pp. 2456 –2466, Sep. 2011.
[8] Corventis. Wireless cardiovascular solutions. (Nov. 2011) [Online]. Available: http://www.corventis.com/us/nuvant.asp
[9] E. Candes, J. Romberg, and T. Tao, "Robust uncertainty principles: Exact signal reconstruction from highly incomplete frequency information," *IEEE Trans. Inform. Theory*, vol. 52, no. 2, pp. 489–509, Feb. 2006.
[10] M. Vetterli, P. Marziliano, and T. Blu, "Sampling signals with finite rate of innovation," *IEEE Trans. Signal Process.*, vol. 50, no. 6, pp. 1417–1428, Jun. 2002.
[11] H. Feichtinger, J. Príncipe, J. Romero, A. Singh Alvarado, and G. Velasco, "Approximate reconstruction of bandlimited functions for the integrate and fire sampler," *Adv. Comput. Math.*, vol. 36, pp. 67–78, 2012.
[12] A. Alvarado, J. Principe, and J. Harris, "Stimulus reconstruction from the biphasic integrate-and-fire sampler," in *Proc. 4th Int. IEEE/EMBS Conf. Neural Eng.*, May 2009, pp. 415–418.
[13] M. Rastogi, A. Singh Alvarado, J. G. Harris, and J. C. Principe, "Integrate and fire circuit as an ADC replacement," in *Proc. IEEE Int. Symp.Circuits Syst.*, May 2011, pp. 2421–2424.
[14] P. de Chazal and R. Reilly, "A patient-adapting heartbeat classifier using ECG morphology and heartbeat interval features," *IEEE Trans. Biomed. Eng.*, vol. 53, no. 12, pp. 2535–2543, Dec. 2006.
[15] J. Wiens and J. Guttag, "Active learning applied to patient-adaptive heartbeat classification," in *Advances in Neural Information Processing Systems 23*, J. Lafferty, C. K. I. Williams, J. Shawe-Taylor, R. Zemel, and A. Culotta, Eds., 2010, pp. 2442–2450.
[16] Y. H. Hu, S. Palreddy, and W. Tompkins, "A patient-adaptable ECG beat classifier using a mixture of experts approach," *IEEE Trans. Biomed. Eng.*, vol. 44, no. 9, pp. 891 –900, Sep. 1997.
[17] T. Ince, S. Kiranyaz, and M. Gabbouj, "A generic and robust system for automated patient-specific classification of ECG signals," *IEEE Trans. Biomed. Eng.*, vol. 56, no. 5, pp. 1415–1426, May 2009.
[18] A. L. Goldberger, L. A. N. Amaral, L. Glass, J. M. Hausdorff, P. C. Ivanov, R. G. Mark, J. E. Mietus, G. B. Moody, C.-K. Peng, and H. E. Stanley, "PhysioBank, PhysioToolkit, and PhysioNet: Components of a new research resource for complex physiologic signals," *Circulation*, vol. 101, no. 23, pp. e215–e220, Jun. 13, 2000.
[19] G. D. Clifford, F. Azuaje, and P. McSharry, *Advanced Methods And Tools for ECG Data Analysis*. Norwood, MA: Artech House, Inc., 2006.
[20] P. de Chazal, M. O'Dwyer, and R. Reilly, "Automatic classification of heartbeats using ECG morphology and heartbeat interval features," *IEEE Trans. Biomed. Eng.*, vol. 51, no. 7, pp. 1196–1206, Jul. 2004.
[21] G. D. Clifford, F. Azuaje, and P. McSharry, *Advanced Methods And Tools for ECG Data Analysis*. Norwood, MA: Artech House Publishers, 2006.
[22] Association for the Advancement of Medical Instrumentation and A. N. S. Institute, *Testing and Reporting Performance Results of Cardiac Rhythm and ST-Segment Measurement Algorithms* (ANSI/AAMI Series) The Association, 1999.
[23] A. A. Lazar, "Time encoding with an integrate-and-fire neuron with a refractory period," *Neurocomputing*, vol. 58–60, pp. 53–58, Jun. 2004.
[24] A. A. Lazar, E. A. Pnevmatikakis, and Y. Zhou, "Encoding natural scenes with neural circuits with random thresholds," *Vision Res.*, vol. 50, no. 22, pp. 2200–2212, Oct. 2010 (special Issue on Mathematical Models of Visual Coding).
[25] A. S. Alvarado, M. Rastogi, J. G. Harris, and J. C. Principe, "The integrate-and-fire sampler: A special type of asynchronous x03a3;–x0394; modulator," in *Proc. IEEE Int. Symp. Proc. Circuits Syst.*,, May 2011, pp. 2031–2034.
[26] A. Alvarado and J. Principe, "From compressive to adaptive sampling of neural and ECG recordings," in *Proc. IEEE Int. Conf. Acoust., Speech Signal Process.*, May 2011, pp. 633–636.
[27] D. J. Daley and D. Vere-Jones, *An Introduction to the Theory of Point Processes*. vol. 1, 2nd, New York: Springer-Verlag, Nov. 2002.
[28] A. R. C. Paiva, I. Park, and J. C. Príncipe, "A reproducing kernel hilbert space framework for spike train signal processing," *Neural Comput.*, vol. 21, no. 2, pp. 424–449, 2009.
[29] F. Rieke, D. Warland, and Rob, W. Bialek, *Spikes: Exploring the Neural Code*, 1st ed. ed. Cambridge, MA: MIT Press, 1997.
[30] T. Sauer, "System identification for chaotic integrate-and-fire dynamics," *Int. J. Intell. Syst.*, vol. 12, no. 4, pp. 255–265, 1997.
[31] T. Sauer, "Reconstruction of dynamical systems from interspike intervals," *Phys. Rev. Lett.*, vol. 72, pp. 3811–3814, Jun. 1994.
[32] M. C. W. van Rossum, "A novel spike distance," *Neural Comput.*, vol. 13, no. 4, pp. 751–763, 2001.
[33] J. D. Victor and K. P. Purpura, "Metric-space analysis of spike trains: Theory, algorithms and application," *Netw.: Comput. Neural Syst.*, vol. 8, no. 2, pp. 127–164, 1997.
[34] J. Principe and J. C. Sanchez, *Brain Machine Interface Engineering*, 1st ed. Seattle, WA: Morgan & Claypool Publishers, 2006.
[35] "Ecg arrhythmia recognition via a neuro-svmäìknn hybrid classifier with virtual qrs image-based geometrical features," *Expert Syst. Appl.*, vol. 39, no. 2, pp. 2047–2058, 2012.
[36] I. Nejadgholi, M. H. Moradi, and F. Abdolali, "Using phase space reconstruction for patient independent heartbeat classification in comparison with some benchmark methods," *Comput. Biol. Med.*, vol. 41, no. 6, pp. 411–419, 2011.
[37] H.-L. Chan, S.-C. Fang, P.-K. Chao, C.-L. Wang, and J.-D. Wei, "Phase-space reconstruction of electrocardiogram for heartbeat classification," in *World Congress on Medical Physics and Biomedical Engineering, September 7–12, 2009, Munich, Germany*. vol. 25/4, (IFMBE Proceedings Series), O. Dossel, W. C. Schlegel, and R. Magjarevic, Eds. Berlin/Heidelberg, Germany: Springer-Verlag, 2010, pp. 1234–1237.
[38] C. M. Bishop, *Pattern Recognition and Machine Learning (Information Science and Statistics)*. Secaucus, NJ: Springer-Verlag, Inc., 2006.
[39] K. Kanoun, H. Mamaghanian, N. Khaled, and D. Atienza, "A real-time compressed sensing-based personal electrocardiogram monitoring system," in *Proc. Design, Autom. Test Eur. Conf. Exhib.*, 2011, Mar., pp. 1–6.
[40] L. Polania, R. Carrillo, M. Blanco-Velasco, and K. Barner, "Compressed sensing based method for ECG compression," in *Proc. IEEE Int. Conf. Acoust., Speech Signal Process.*, May 2011, pp. 761–764.
[41] Y. Hao, P. Marziliano, M. Vetterli, and T. Blu, "Compression of ECG as a signal with finite rate of innovation," in *Proc. 27th Annu. Int. Conf. Eng. Med. Biol. Soc.*, Jan. 2005, pp. 7564–7567.

Alexander Singh Alvarado received the B.Sc. degree in electrical engineering from the Instituto tecnológico de Costa Rica, Cartago, Costa Rica, in 2006, and the M.Sc. and Ph.D. degrees in electrical engineering from the University of Florida, Gainesville, in 2008 and 2012, respectively.

He is a technology consultant at Hewlett-Packard in Palo Alto, CA. His research interests include adaptive sampling, machine learning, statistical signal processing and computational neuroscience.

Choudur Lakshminarayan received the Ph.D. degree in mathematical sciences from the University of Texas.

He is a Principal Research Scientist in the Hewlett-Packard Laboratories, Palo Alto CA. His research interests include mathematical statistics and applied mathematics with applications in large data, compression, pattern analysis, and prediction.

José C. Príncipe (F'00) received degree in electrical engineering from the University of Porto (Bachelor), Portugal, University of Florida (Master and Ph.D.), USA and a Laurea Honoris Causa degree from the Universita Mediterranea in Reggio Calabria, Italy.

He is a Distinguished Professor of Electrical and Biomedical Engineering at the University of Florida, Gainesville. He is a BellSouth Professor and Founding Director of the University of Florida Computational Neuro-Engineering Laboratory (CNEL). His research interests are centered in advanced signal processing and machine learning, brain machine interfaces and the modeling and applications of cognitive systems.

Dr. Príncipe is a Fellow of the AIMBE, past President of the International Neural Network Society, and Past Editor in Chief of the TRANSACTIONS OF BIOMEDICAL ENGINEERING, as well as a former member of the Advisory Science Board of the FDA.